EFFECT OF Nb ADDITION ON COMPACT MICROSTRUCTURE AND MECHANICAL PROPERTIES OF GRAY CAST IRON FOR CYLINDER LINER

Zhuang Li, Yan Zhang and Qiang Song
School of Materials Science and Engineering, Shandong University of Science and Technology, Qingdao 266500, People's Republic of China

Ruirun Chen
School of Materials Science and Engineering, Shandong University of Science and Technology, Qingdao 266500, People's Republic of China
National Key Laboratory for Precision Hot Processing of Metals, School of Materials Science and Engineering, Harbin Institute of Technology, Harbin 150001, People's Republic of China

Qi Wang and Chaoyang Chen
National Key Laboratory for Precision Hot Processing of Metals, School of Materials Science and Engineering, Harbin Institute of Technology, Harbin 150001, People's Republic of China

https://doi.org/10.1007/s40962-024-01292-x

Abstract

To improve the mechanical properties and the strengthening mechanism, gray cast irons (Nb content is 0 wt.%, 0.15 wt.%, 0.2 wt.%, 0.25 wt.%, 0.3 wt.%, and 0.35 wt.%, simplify as Nb0, Nb1.5, Nb2, Nb2.5, Nb3, Nb3.5, respectively) were prepared using a medium-frequency induction furnace. The results show that the interlamellar spacing in the microstructure of the gray cast iron matrix is refined by the addition of Nb, and the spacing decreases from 530 nm to 210 nm. The A-type graphite decreases in size and gets distributed more homogeneously. With the addition of Nb, the Vickers hardness and tensile strength of the gray cast iron increases. The Nb2.5 has excellent structural uniformity and refines the pearlite spacing to 210 nm, showing stable mechanical properties. The Nb3.5 gray cast iron exhibits the best mechanical properties, the Vickers hardness and tensile strength are 389 HV and 537 MPa, respectively. The improvement in Vickers hardness and tensile strength is attributed to second-phase strengthening, solid solution strengthening, and fine-grain strengthening. This work will provide experience for the material design of high-performance gray cast iron cylinder liners.

Keywords: *gray cast iron, alloying, pearlite, mechanical properties, microstructure, cylinder liners, niobium, Nb*

Introduction

The demand for materials with high-strength and wear-resistance has never waned in engineering applications and scientific research. With the internal combustion engine industry rapidly developing, engines are faced with increasingly demanding service environments that involve higher temperatures and complex stress. Consequently, the service life and capacity of engines are required to meet higher standards.[1,2] The behavior of the cylinder liner's movement is crucial in determining the internal combustion engine's fuel consumption, emissions, and mechanical efficiency.[3–5] Therefore, cylinder liners demand superb material tensile strength, wear resistance, and hardness, while balancing the economic viability of the production process. As a consequence, gray cast iron with pearlite as the primary structure remains the most frequently chosen material to date.[6–12] Alloying can be employed as an effective technique to enhance the performance of materials, such as precipitation strengthening, fine-grain strengthening, and solid solution strengthening through doping alloying elements.[13–18]

Received: 08 November 2023 / Accepted: 03 February 2024
Published online: 18 March 2024

Adding Nb to gray cast iron can improve its mechanical properties due to its significant effect on the morphology of the graphite flake and the microstructure of the matrix. The Nb reacts with carbon before solidification to generate fine NbC particles. It can serve as the germination center for graphite, resulting in the enhancement of graphite's refinement and eutectic clusters. In addition, the presence of Nb solid solution within the matrix results in the solid solution strengthening. What is more, it forms Nb-rich phases at grain boundaries, which is typically the major form of Nb in cast iron.[19–23] A large number of studies indicate that Nb has a significant ability to refine pearlite and assist its formation.[24–26] Zhou et al.[28] examined the impact of Nb alloying on materials of high carbon equivalent gray cast iron. Thermodynamic calculations indicate that the formation of NbC phase preceded the eutectic transformation. The result indicates that the inclusion of Nb up to a certain threshold modifies the microstructure of graphite and eutectic clusters. Moreover, pearlite interlamellar spacing decreases, caused by lowering the eutectoid temperature.

In this work, to obtain a gray cast iron with high Vickers hardness and tensile strength, the gray cast irons with different Nb contents (Nb=0 wt.%, 0.15 wt.%, 0.2 wt.%, 0.25 wt.%, 0.3 wt.%, and 0.35 wt.%) were prepared by medium-frequency induction furnace, the microstructure was observed and the mechanical properties were tested, with an aim to find optimum addition of Nb and to provide information for increased production of high-quality gray cast iron as large cylinder liners.

Experimental Procedure

Due to the high melting point of Nb, ferro-niobium was chosen as the source of alloying elements. Melt the material in a 10-kg capacity medium-frequency induction furnace. The samples were inoculated using the barium silicon inoculant supplied by Yixing Jiahu Furnace Charge Co., Ltd. The molten iron was poured into the ladle at 1650–1750 K. Add the inoculant to the molten iron, let it stand for one minute, and skim off the surface slag. Pour molten iron into the preheating mold made of silica chemically bonded sand. Every single specimen is weighed separately and then put into the furnace for casting. The microstructural examination and mechanical analysis sections were taken from the upper part of the shaded area in Figure 1(a), which shows the dimensions of the Y-shaped specimens.

The cast alloys were chemically characterized and the results are shown in Table 1. Metallographic specimens measuring 10 mm × 10 mm × 10 mm. These specimens were then sanded and polished using various grades of sandpaper. The physical properties of the polished surfaces were analyzed using an X-ray diffractometer, with Cu Kα utilized for diffraction. Scanning was carried out at an angle between 20° and 100°, and the scanning speed was at 5 min.$^{-1}$ Then etched with 4 % nital (4 mL HNO3 + 96 mL ethanol) to observe the microstructures with field emission scanning electron microscopy (FE-SEM; Hitachi TM4000) at 15 Kv and Olympus GX71 Optical Microscope (OM). Nano measurer software was used to randomly select five adjacent pearlites from the same image for measurement, and obtain the average value. To reduce errors, the above process is repeated three times to obtain the final result. An analysis was conducted on the phase or microstructure, using Image Pro Plus 6.0, with a focus on quantitative measurements.

The sample's hardness was evaluated using a microhardness tester, under 1 kg load holding for 10 s. To reduce experimental error, each sample was measured five times, and the mean value was used as the experimental outcome. According to ASTM A247, the specimen used for tensile testing has a scale length of 30 mm and a scale width of 6 mm, as shown in Figure 2. The specimens were pulled at a rate of 1 mm/min under a strain rate of 10^3/s. Each group was tested thrice.

Results and Discussion

Phase Analysis

The X-ray diffraction patterns of the standard cast iron and the cast iron with a 0.2 wt.% Nb addition are presented in Figure 3. Figure 3b shows that residual austenite is formed alongside ferrite in the gray cast iron structure as a result of the inclusion of the Nb element. According to the analysis of powder diffraction file (PDF) cards, the lattice constant of ferrite has increased from 2.869 Å to 2.872 Å. The reason for this phenomenon is as follows: after adding Nb, the atomic radius of Nb is larger than that of iron atoms, and it solidly dissolves in ferrite, causing its lattice constant to increase.

Microstructural Characterization

The morphology of graphite in gray cast iron samples with varying Nb concentrations is depicted in Figure 4 before corrosion. Figure 4 shows that the graphite morphology of gray cast iron without Nb addition was predominantly A-type graphite, the graphite flake is thicker and the distribution of organization is not good. There is an increase in the amount of graphite, accompanied by a refinement in its morphology, curvature, and distribution uniformity, when the Nb content reaches 0.2 wt.%. When Nb content is 0.35 % by weight, less graphite forms, as shown as Table 2.

The reduction in graphite area with Nb doping and refinement occurs for three primary reasons. Firstly, Nb can

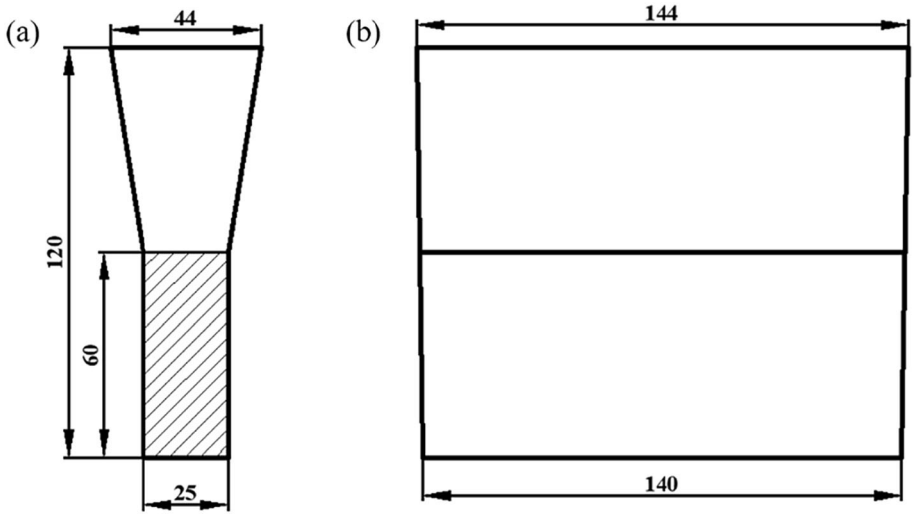

Figure 1. Dimensions of Y-block mold: (a) Main view; (b) Left view.

Table 1. Chemical Compositions of Experimental Iron

Alloys	C	Si	Mn	P	S	Nb	Fe
Nb0	2.95	2.11	0.71	0.23	0.05	0	Bal.
Nb1.5	3.02	1.83	0.68	0.23	0.04	0.16	Bal.
Nb2	3.13	2.05	0.77	0.26	0.02	0.19	Bal.
Nb2.5	2.98	1.96	0.63	0.24	0.05	0.27	Bal.
Nb3	3.05	2.06	0.73	0.21	0.03	0.30	Bal.
Nb3.5	2.93	2.13	0.64	0.28	0.06	0.36	Bal.

lower eutectic transition temperature so that the diffusion ability of carbon atoms is reduced. Secondly, Nb atoms have a strong bond to C atoms, which leads to difficulties in the diffusion of carbon atoms, making it difficult for graphite to grow.[27,28] Finally, due to its strong tendency to form carbides and nitrides, Nb combines with carbon to form a fine Nb-rich phase in ferro-water before solidification.

Figure 5 shows the morphology of the matrix structure of samples with different Nb contents after corrosion. The matrix structure of gray cast irons is pearlitic and all show

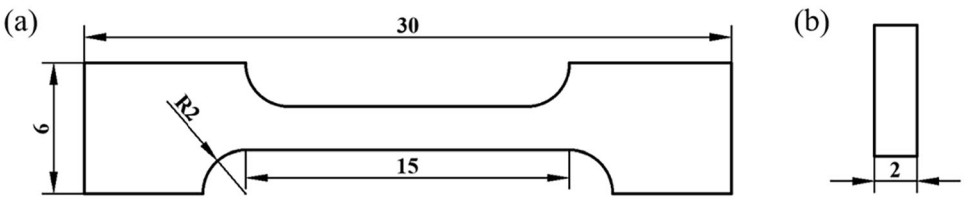

Figure 2. Dimensions of Y-block mold: (a) Main view; (b) Side view.

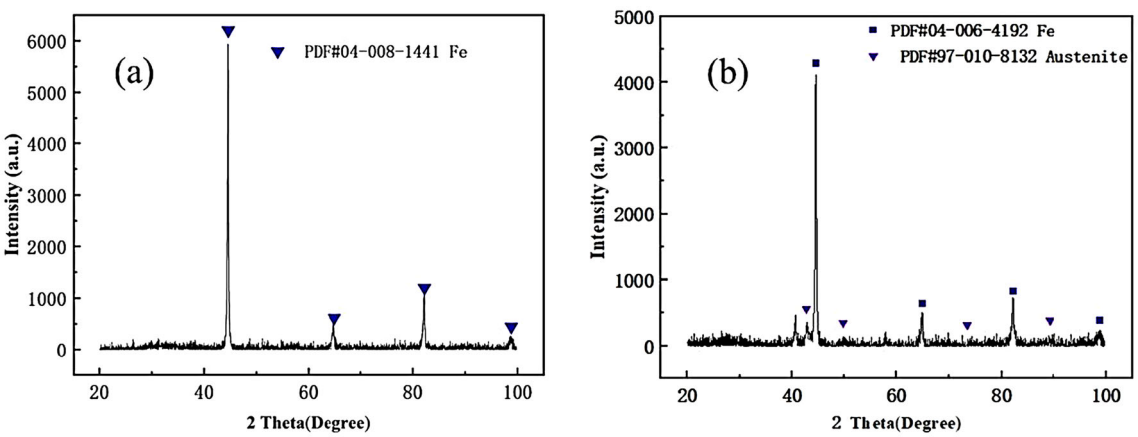

Figure 3. X-ray diffraction patterns of cast iron: (a) 0 wt.% Nb; (b) 0.2 wt.% Nb.

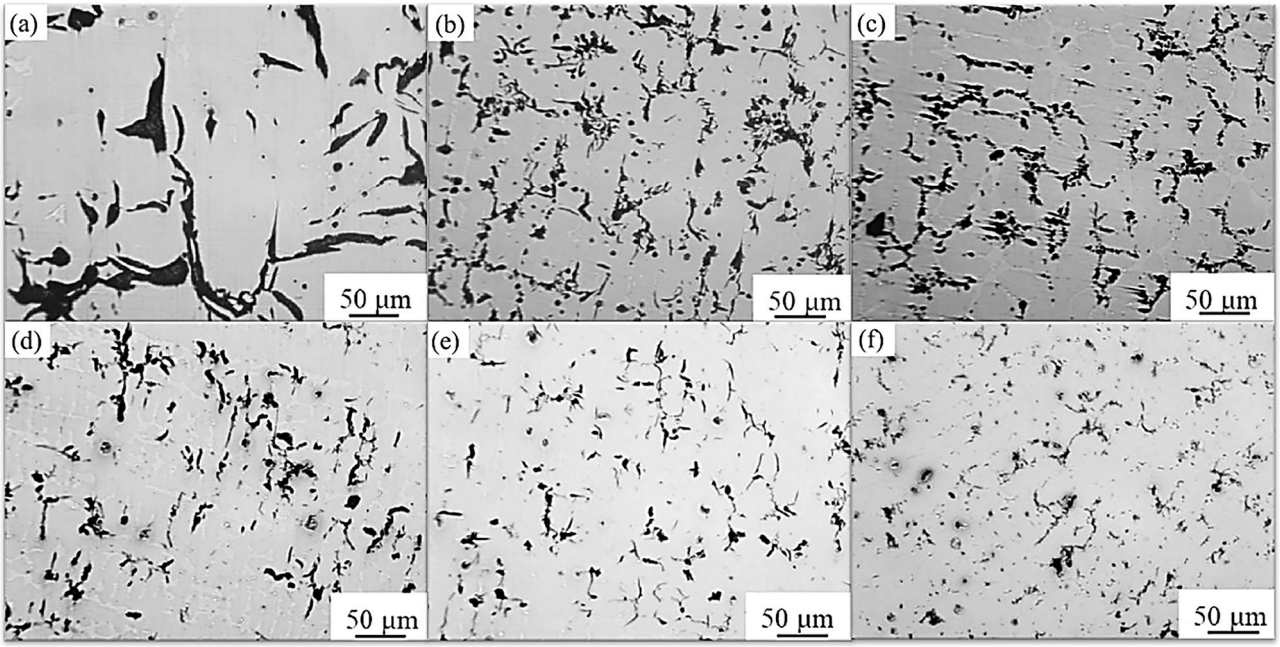

Figure 4. Microstructure and graphite morphology of gray cast iron specimens with different Nb contents: (a) 0 wt.% Nb; (b) 0.15 wt.% Nb; (c) 0.2 wt.% Nb; (d) 0.25 wt.% Nb; (e) 0.3 wt.% Nb; (f) 0.35 wt.% Nb.

Table 2. Summary of Microstructural Features

Alloys	Graphite type	Graphite area (μm^2)	Graphite area ratio (%)	Pearlite content (nm)
Nb0	A	7.235×10^4	15.48	530
Nb1.5	A	6.567×10^4	14.45	360
Nb2	A	6.248×10^4	13.32	240
Nb2.5	A	4.144×10^4	11.07	210
Nb3	A	3.317×10^4	10.47	270
Nb3.5	A	2.941×10^4	10.21	280

lamellar pearlitic organization containing ferrite and a small amount of phosphorus eutectic. The addition of Nb element has little effect on the pearlite content, which is 90 % to 92 %.

Figure 6 illustrates the matrix organization morphology of gray cast iron samples containing varying amounts of Nb, analyzed under a scanning electron microscope. As illustrated in Figure 6, the addition of Nb doping results in the emergence of square, rhombic, and irregularly shaped bright white precipitates in the structure of cast iron. It is notable that such phases increase in concentration as the Nb content grows. The energy dispersive X-ray spectroscopy (EDS) analysis revealed the precipitated phase as a complex carbon-nitrogen compound containing Nb. Nb has limited solubility in iron-based alloys, which results in the formation of hard phases like NbC, NbN, or the composite Nb(C, N) when added in amounts exceeding its solubility in the ferrofluid.

When the dislocations within the structure of the matrix shift, the more rigid precipitated phases that are scattered throughout the matrix will significantly impede the process and enhance the mechanical characteristics. Simultaneously, the microhardness of carbonitrides proves to be exceptionally high, ranging from 2300 to 2500 HV. As a result, the wear resistance of the sliding friction of the material has been improved.[29]

Figure 7 displays the pearlitic structure of gray cast iron samples containing varying amounts of Nb. The findings indicate that with increase in Nb content, the spacing between the pearlitic lamellae decreases initially and then stabilizes, as evidenced in Figure 8. The transformation from austenite to ferrite is a comparatively simple process since the iron atoms within the austenitic lattice can move swiftly, thus converting austenite to ferrite with ease. However, the process of transforming to carburize is challenging. Therefore, the main reason for the change in the spacing of the pearlite layers can be understood in the following way. Firstly, the Nb element can increase the degree of supercooling during eutectic transformation, which prevents carburization and ferrite from growing sufficiently. Secondly, the presence of Nb in a solid solution inhibits carbon atom diffusion, ultimately leading to a reduction in pearlite lamellar spacing over time.[30] As the Nb content increases, more Nb-rich phases precipitate first in the matrix. This phenomenon consumes more Nb atoms, reducing the number of Nb atoms dissolved in the matrix. Therefore, during the eutectoid transformation, a small

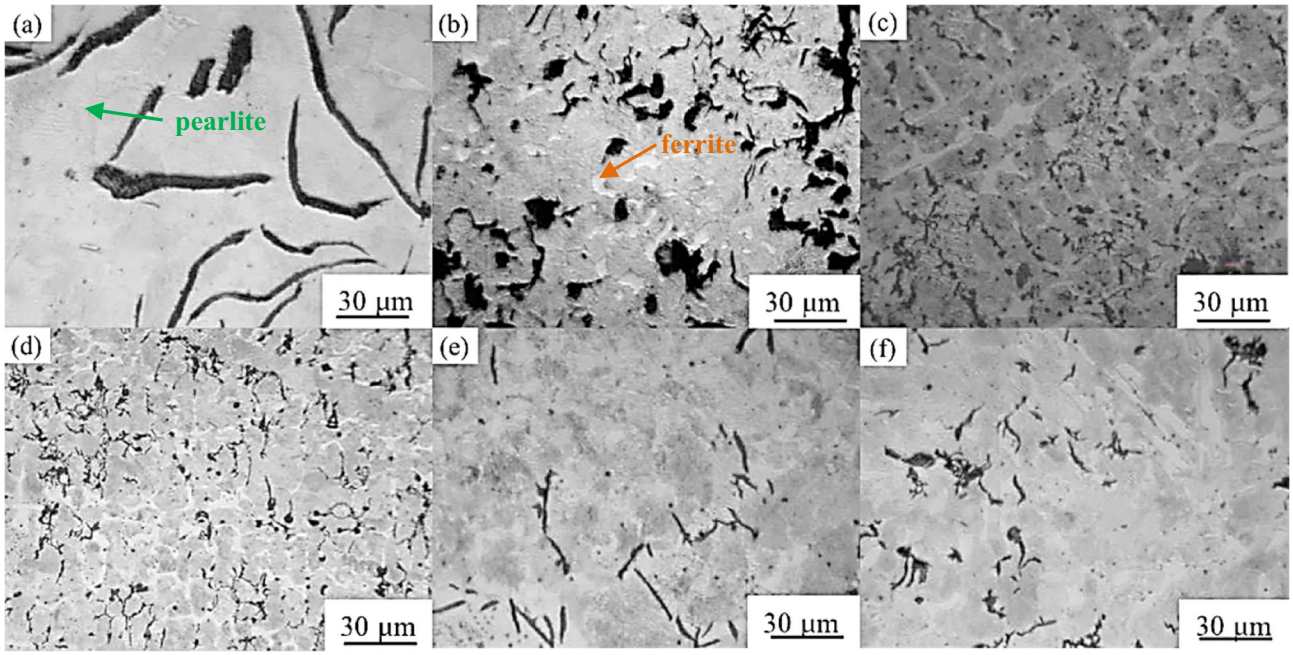

Figure 5. OM structure of the cast irons with different contents of Nb: (a) 0 wt.% Nb; (b) 0.15 wt.% Nb; (c) 0.2 wt.% Nb; (d) 0.25 wt.% Nb; (e) 0.3 wt.% Nb; (f) 0.35 wt.% Nb.

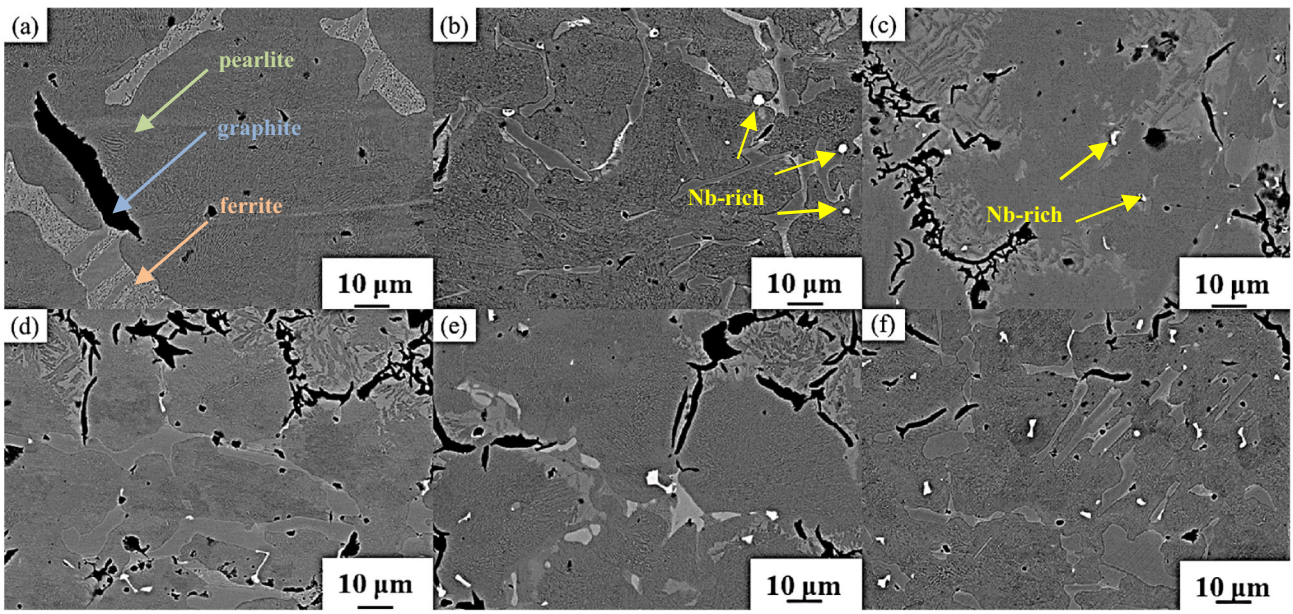

Figure 6. SEM structure of the cast irons with different contents of Nb: (a) 0 wt.% Nb; (b) 0.15 wt.% Nb; (c) 0.2 wt.% Nb; (d) 0.25 wt.% Nb; (e)0.3 wt.% Nb; (f) 0.35 wt.% Nb.

amount of Nb hinders the diffusion of carbon atoms, causing a slight increase in the lamellar spacing of pearlite.

Meanwhile, it is evident from Figure 7e that the pearlite lamellae exhibit distinct orientations on both sides of the bulk NbC, demonstrating that the majority of the Nb-rich phases form along the grain boundaries of the eutectic clusters or subgranular boundaries within the eutectic clusters. This is due to the area having a higher concentration of Nb atoms, which creates concentration undulations and facilitates the formation of NbC. The amalgamation of Nb and carbon in the final phase of solidification is suggested by the formation of Nb-rich phases in the vicinity of eutectic clusters. This process prevents the formation of bulky carbides and phosphorus eutectics by utilizing carbon atoms in the final solidification region. Thus, substantial carbide and phosphorus eutectic will become finer, resulting in a stronger bond at the boundary of the eutectic clusters. This can inhibit the expansion of cracks along the grain boundaries, thereby

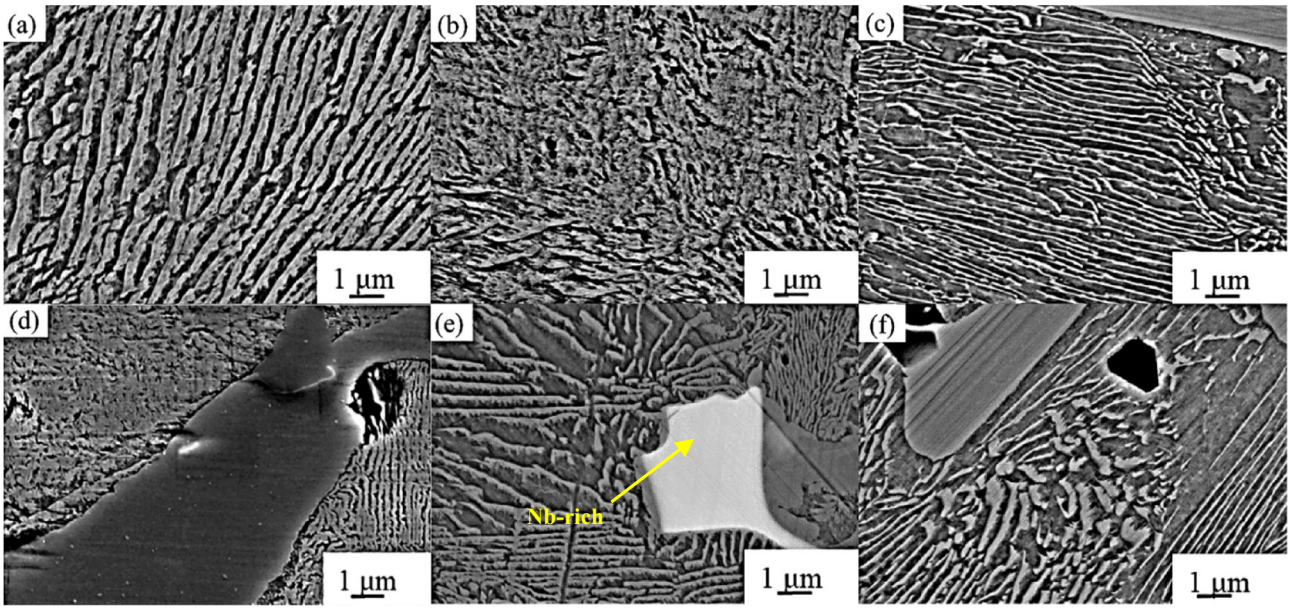

Figure 7. Pearlite organization of gray cast iron specimens with different Nb contents: (a) 0 wt.% Nb; (b) 0.15 wt.% Nb; (c) 0.2 wt.% Nb; (d) 0.25 wt.% Nb; (e) 0.3 wt.% Nb; (f) 0.35 wt.% Nb.

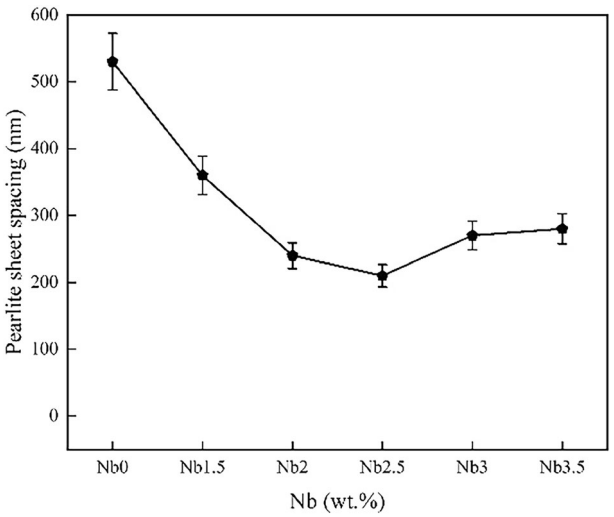

Figure 8. Pearlite sheet spacing of the cast irons with different contents of Nb.

enhancing the strength, toughness, and fatigue resistance of gray cast iron. It is proven to improve matrix strength, microhardness, and wear resistance of cast irons. This enhances the material's resistance to deformation while also decreasing the likelihood of crack expansion and propagation in the matrix.

It is clear from Figure 9 that the iron is uniformly dispersed within the matrix organization. Most of the carbon exists as graphite, with a small proportion evenly distributed and dissolved in the ferrite matrix, while a further small amount forms cementite. While phosphorus is mainly present in the form of phosphorus eutectic, silicon is evenly distributed throughout the matrix of the medium. The distribution of manganese and sulfur indicates that most of these elements are distributed evenly throughout the matrix organization. However, a slight portion of the MnS mixture takes the form of micro-areas which can be observed in the micro-area of Nb. The enrichment of S elements in this area contributes to the formation of a certain kind of Nb-rich complex phases. The EDS/SEM results show that the Nb-rich phase is a large amount of NbC, as shown in Table 3. During the reaction, some small NbC particles may merge to form a block. However, in the cooling process, some small NbC particles will inevitably remain. These particles act as a graphite nucleus core in the eutectic reaction, which enhances the nucleation rate. This leads to the refinement of graphite.[31,32]

Mechanical Properties

As shown in Figure 10a, a rise in Nb concentration leads to an increase in the tensile strength of gray cast iron with an upward trend. The tensile strength of Nb0 cast iron is 311 MPa. When the addition amount is 0.15 wt.%, the strength increases to 395 MPa, a 27 % increase compared to the specimen without the added Nb element. The maximum tensile strength attained by the gray cast specimen is 537 MPa with an Nb content of 0.35 wt.%. The impact of Nb content on the tensile strength of gray cast iron castings is highly significant. This is because when a cast iron specimen is subjected to a tensile force, the ferrite, being soft, deforms initially while the carburite phase, which is hard and brittle, prevents the movement of dislocations, allowing them to shift only a limited distance. The higher the quantity of dislocations amid the pearlite layers, the greater the external force required to deform the cast iron

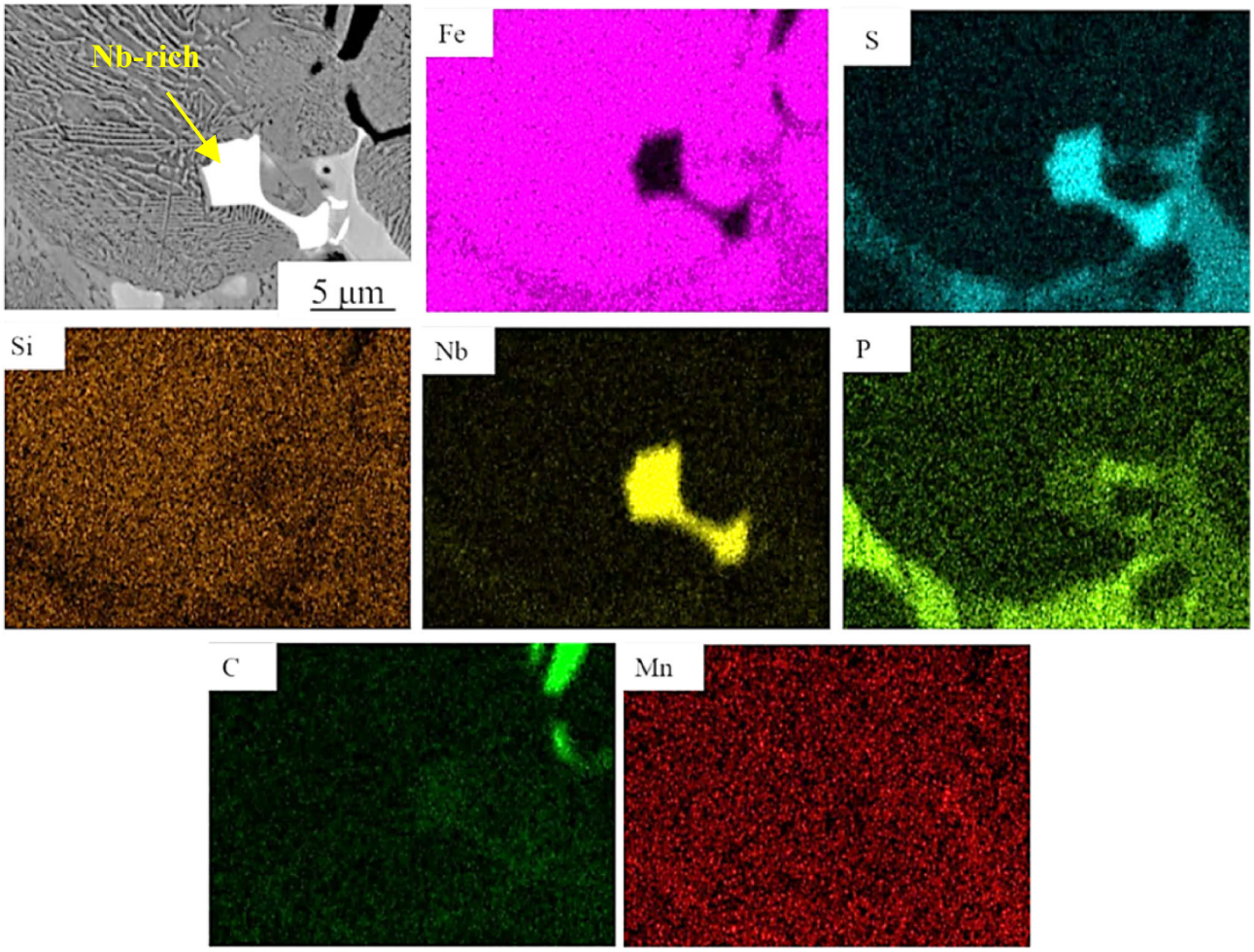

Figure 9. Results of the surface scanning energy spectrum analysis of the sample with 0.3 wt.% Nb.

Table 3. Chemical Compositions (at.%) of Rich Nb Phase

	C	Si	Mn	Nb	S	Fe
NbC	46.95	2.14	2.24	39.93	5.92	2.81

material. By reducing the spacing between sheet layers, pearlescent organization's uniformity will improve, resulting in better uniformity in cast iron deformation. A homogeneous microstructure reduces the risk of fracture and significantly enhances its mechanical properties.

Figure 10b displays the mean and standard deviation of the microhardness of cast iron samples with varying Nb contents. The eutectic transformation of gray cast iron results in different pearlitic and ferrite organizations with varying dispersion degrees of Nb content, leading to a difference in the microhardness of the matrix organization in different regions. Consequently, the microhardness of the cast iron samples with different Nb contents varies. Furthermore, the deviation of microhardness was used to indicate the consistency of the matrix structure. The variability in microhardness demonstrated diverse tendencies, as the standard deviation of microhardness of gray cast iron specimens initially decreased, followed by an increase with the rise in Nb content. Notably, the addition of 0.25 wt.% of the gray cast iron specimen was another significant factor. The microhardness standard deviation was lowest for Nb2.5 cast iron and indicating greater structural consistency.

The phenomenon occurs because of the presence of a certain amount of Nb in steel materials, resulting in solid solution strengthening. This, in turn, leads to lattice distortion and the generation of an interactive stress field. From an atomic size perspective, Nb exhibits a 9.8 % difference in atomic radius compared to both γ-Fe and α-Fe. This indicates a favorable basis for the formation of larger solid solutions as the difference between them is less than 15 %. From an electronegativity standpoint, the electronegativity of Nb is comparable to that of Fe, while the electronegativity of Nb shows a significant variation from that of the nonmetallic elements C, N, and O. The similarity in electronegativity between Nb and Fe enables

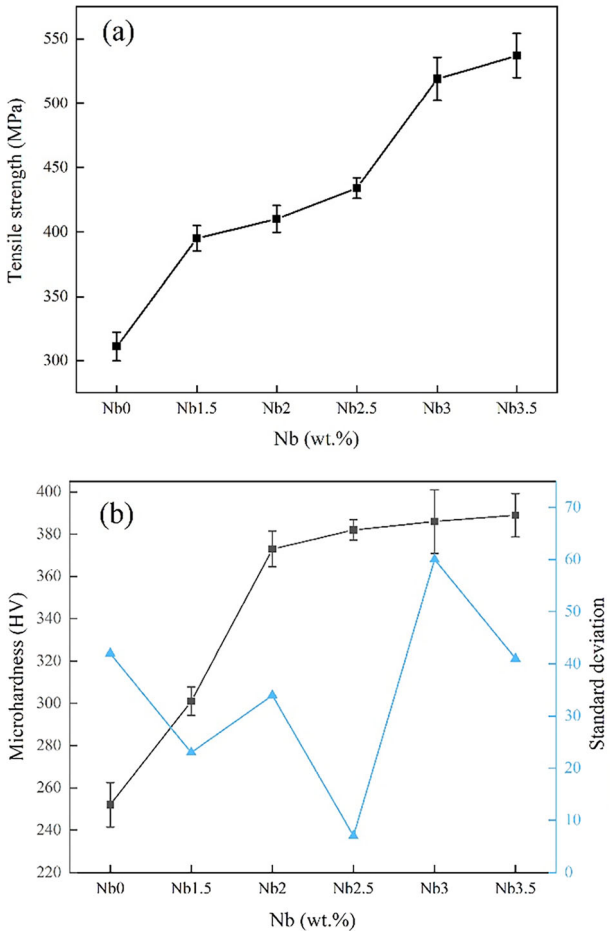

Figure 10. Effect of Nb content on mechanical properties: (a) Tensile Strength; (b) Microhardness and Standard Deviation.

Nb to act as a solid solution in the iron matrix. It can also combine with nonmetal elements like carbon, nitrogen, and oxygen to form compounds or solid solutions. These can function as evenly distributed dual-phase strengtheners within the matrix structure to enhance the overall mechanical attributes of cast iron.[33,34]

Furthermore, the wear resistance of cast iron materials is improved by the increased hardness of the reinforced phase plasmas distributed throughout the matrix. Firstly, the use of graphite in cast iron can serve as a lubricant, storing lubricant and sustaining the continuity of the lubricating film. In the event of friction-shedding cavities, graphite can further store lubricant, thereby enhancing the wear resistance of gray cast iron. After undergoing frictional damage, the elevated hardness of the hard points in the gray cast iron will ascend gradually above the surface. Consequently, a primary sliding surface will be formed, whereas the relatively soft graphite and pearlite matrix will form a secondary sliding surface. Moreover, hard phase mass demonstrates considerable hardness and diminishes the contact surface area between the sample and the frictional element, thereby conferring outstanding wear-resistance capabilities.

When a cast iron specimen is subjected to tensile force, the ferrite, being softer, deforms first while the carburized body, harder and more brittle, acts as a barrier to prevent dislocation movement. Consequently, dislocations are only able to move over very short distances. The magnitude of the force required to deform the cast iron is increased by the amount of dislocations present in the pearlite. This results in enhanced plastic deformation resistance, leading to an overall improvement in the mechanical characteristics of cast iron. Finally, decreasing the distance between the lamellae will enhance the uniformity of the pearlite arrangement and homogenize the cast iron's deformation, lowering the risk of fracture. Consequently, this significantly augments cast iron's deformation ability.

As shown in Figure 11, the tensile fracture consists mainly of cleavage surface with a clear fan-shaped expansion outward, forming a river-like pattern. As the Nb content increases, there is a secondary fragmentation that creates a stepped structure, as indicated by the arrow. The specimen with lower Nb content exhibits a significantly lower number of tear ribs on its fracture compared to the specimen with higher Nb content. This is due to Nb-rich carbonnitride Nb(C, N) hard dots embedded within the matrix.[33–35] These hard dots act as dislocation pins, effectively hindering dislocation movement, thus achieving the desired result.

The fracture of cast iron specimens under tensile conditions is primarily caused by the graphite and brittle phases within it. Tensions cause brittle fractures to initiate on the flake graphite. The distribution of graphite in cast iron lacking the Nb element is coarse and uneven, rendering it vulnerable to fracture when subjected to tensile stress. The fractures propagate along disintegration surfaces and phase interfaces, eventually culminating in a brittle disintegration fracture of the cast iron. After adding Nb elements, the graphite flakes in the structure become finer and more evenly distributed, reducing the likelihood of bending and crack propagation. The matrix also experiences reduced tearing, making it less prone to large-scale surface disintegration. As a consequence, the mechanical characteristics of cast iron undergo a substantial improvement.

Conclusions

In this work, microstructure evolution and mechanical properties with different Nb doping are systematically estimated, and corresponding conclusions are as follows:

(1) As the Nb content increases, the graphite in the microstructure is fine and homogeneous. The change of graphite quantity is not obvious, and

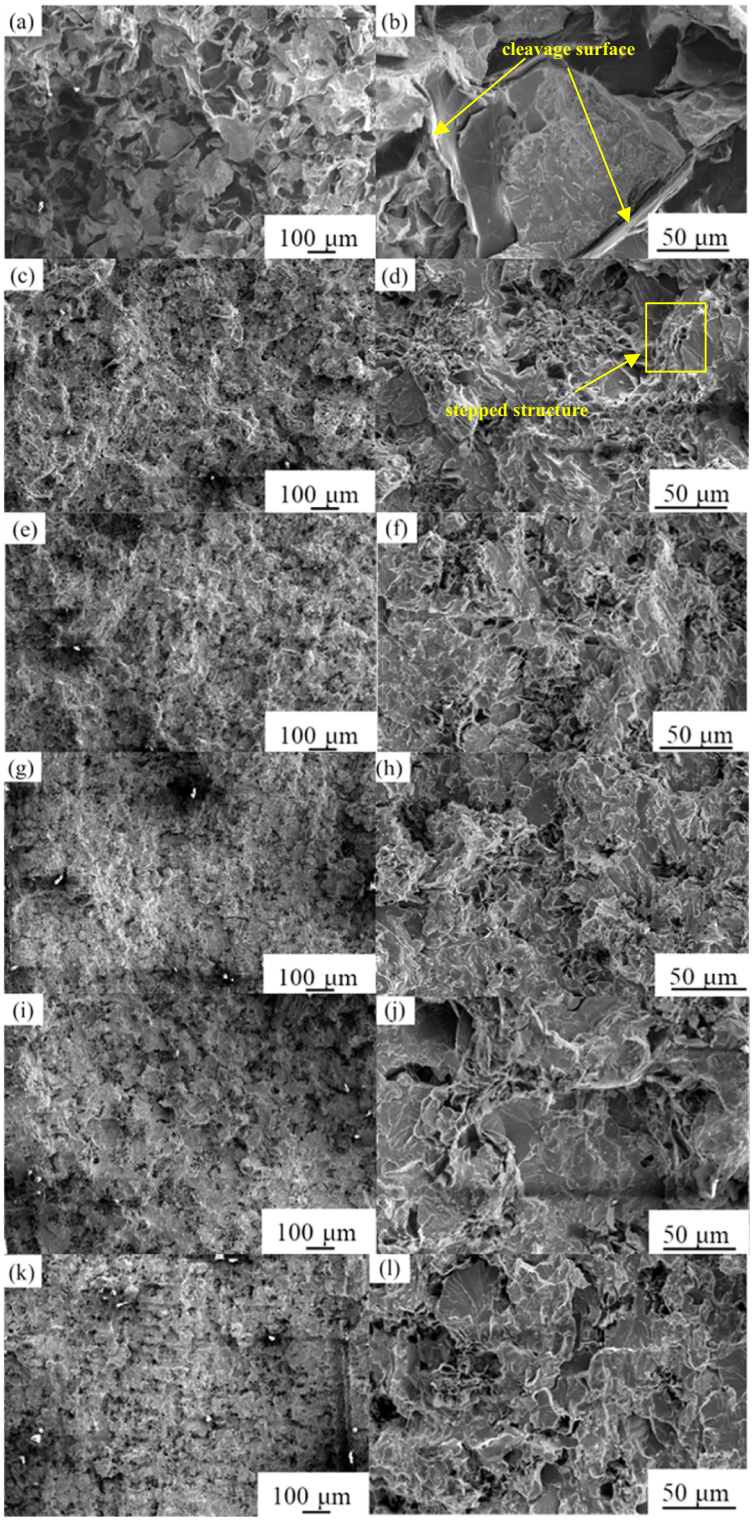

Figure 11. Tensile fracture morphology of gray cast iron castings with different Nb contents: (a, b) 0 wt.% Nb; (c, d) 0.15 wt.% Nb; (e, f) 0.2 wt.% Nb; (g, h) 0.25 wt.% Nb; (i, j) 0.3 wt.% Nb; (k, l) 0.35 wt.% Nb.

the sheet spacing between pearlite decreases gradually because of the increase of Nb content. The more Nb added, the more Nb-rich phases appear, which is diffusely distributed in the matrix. Its shapes include square, irregular strips, etc. Besides the Nb-rich carbides embedded in the matrix, Nb element is mainly dissolved in gray cast iron.

(2) The hardness standard deviation of cast iron specimens exhibits an initial decrease followed by an increase. Introducing 0.25 wt.% of gray cast iron results in the lowest microhardness standard deviation, indicating superior microstructure uniformity. With the Nb content increase, the tensile strength and hardness of gray cast irons improve, which is owning to second-phase strengthening, solid solution strengthening, and fine-grain strengthening. Nb3.5 has the best mechanical properties, the Vickers hardness and tensile strength are 389 HV and 537 MPa, respectively.

(3) The fracture morphology displays obvious river pattern, which is a typical brittle fracture feature. Incorporating Nb into the cast iron has reduced the spacing between the pearlitic lamellae and plays a role in refining the graphite. It improves the mechanical properties of cast iron to a certain extent.

Acknowledgements

The authors gratefully acknowledge financial support from the National Natural Science Foundation of China (No. U21A2042) and the National Natural Science Foundation of China (No. 52374384).

REFERENCES

1. M. Javidani, D. Larouche, Application of cast Al–Si alloys in internal combustion engine components. Int. Mater. Rev. **59**(3), 132–158 (2014). https://doi.org/10.1179/1743280413y.0000000027
2. P.-R. Ren, W. Song, G. Zhong et al., High-cycle fatigue failure analysis of cast Al-Si alloy engine cylinder head. Eng. Fail. Anal. (2021). https://doi.org/10.1016/j.engfailanal.2021.105546
3. C. Delprete, A. Razavykia, Piston dynamics, lubrication and tribological performance evaluation: A review. Int. J. Engine Res. **21**(5), 725–741 (2018). https://doi.org/10.1177/1468087418787610
4. M. Cakir, İH. Akcay, Effects of borided cylinder liner on engine performance in a firing diesel engine. Arabian J. Sci. Eng. **40**(11), 3329–3335 (2015). https://doi.org/10.1007/s13369-015-1807-6
5. Y.-L. Li, Q. Wang, R.-R. Chen et al., Influence of V content on microstructure and mechanical properties of gray cast iron for super-large cylinder liner. Inter Metalcast **17**(3), 1806–1814 (2022). https://doi.org/10.1007/s40962-022-00894-7
6. C. Thiagarajan, M. Prabhahar, S. Prakash et al., Heat transfer analysis and optimization of engine cylinder liner using different materials. Mater. Today Proc. **33**, 778–783 (2020). https://doi.org/10.1016/j.matpr.2020.06.173
7. T. Wopelka, U. Cihak-Bayr, C. Lenauer et al., Wear of different material pairings for the cylinder liner – piston ring contact. Ind. Lubr. Tribol. **70**(4), 687–699 (2018). https://doi.org/10.1108/ilt-07-2017-0218
8. S.C. Tung, M.L. McMillan, Automotive tribology overview of current advances and challenges for the future. Tribol. Int. **37**(7), 517–536 (2004). https://doi.org/10.1016/j.triboint.2004.01.013
9. T.V.S. Reddy, D.K. Dwivedi, N.K. Jain, Adhesive wear of stir cast hypereutectic Al–Si–Mg alloy under reciprocating sliding conditions. Wear **266**(1–2), 1–5 (2009). https://doi.org/10.1016/j.wear.2008.05.003
10. G.-Q. Wang, Z.-L. Liu, Y.-X. Li et al., Different thermal fatigue behaviors between gray cast iron and vermicular graphite cast iron. China Found. **19**(3), 245–252 (2022). https://doi.org/10.1007/s41230-022-1204-1
11. T. Murakami, T. Inoue, H. Shimura et al., Damping and tribological properties of Fe-Si-C cast iron prepared using various heat treatments. Mater. Sci. Eng. A **432**(1–2), 113–119 (2006). https://doi.org/10.1016/j.msea.2006.06.090
12. M.C. Rukadikar, G.P. Reddy, Influence of chemical-composition and microstructure on thermal-conductivity of alloyed pearlitic flake graphite cast irons. J. Mater. Sci. **21**(12), 4403–4410 (1986). https://doi.org/10.1007/bf01106563
13. W. Zhai, L. Bai, R. Zhou et al., Recent progress on wear-resistant materials: designs, properties, and applications. Adv. Sci. **8**(11), e2003739 (2021). https://doi.org/10.1002/advs.202003739
14. J. Miao, T. Guo, J. Ren et al., Optimization of mechanical and tribological properties of FCC CrCoNi multi-principal element alloy with Mo addition. Vacuum **149**, 324–330 (2018). https://doi.org/10.1016/j.vacuum.2018.01.012
15. Y.-P. Chang, Z.-W. Huang, H.-M. Chou, Effects of doping elements on the friction and wear of SUJ2 steel sliding against aluminum alloys. Micromachines (2017). https://doi.org/10.3390/mi8040096
16. A. Hassani, A. Habibollahzadeh, S. Sadeghinejad, Influence of vanadium and chromium additions on the wear resistance of a gray cast iron. Int. J. Miner. Metall. **19**(7), 602–607 (2012). https://doi.org/10.1007/s12613-012-0601-7
17. M. Moonesan, A.H. Raouf, F. Madah et al., Effect of alloying elements on thermal shock resistance of gray cast iron. J. Alloys Compd. **520**, 226–231 (2012). https://doi.org/10.1016/j.jallcom.2012.01.027
18. S.O. Omole, K.K. Alaneme, A. Oyetunji, mechanical damping characteristics of ductile and grey irons micro-alloyed with combinations of Mo, Ni, Cu and Cr. Acta Metall. Slovaca. **27**(2), 87–93 (2021). https://doi.org/10.36547/ams.27.2.791
19. G. Beniwal, K.K. Saxena, Effect of niobium addition in grey cast iron: A short review. Mater. Today Proc.

26, 2337–2343 (2020). https://doi.org/10.1016/j.matpr.2020.02.503
20. M.O. Azzoug, N. Boutarek-Zaourar, D. Aboudi et al., Niobium addition effect in molds at last cooling step on EN-GJL250 gray cast iron: Microstructural changes and electrochemical behavior. China Found. **15**(3), 228–235 (2018). https://doi.org/10.1007/s41230-018-8007-4
21. S. Pan, F. Zeng, N. Su et al., The effect of niobium addition on the microstructure and properties of cast iron used in cylinder head. J. Mater. Res. Technol. **9**(2), 1509–1518 (2020). https://doi.org/10.1016/j.jmrt.2019.11.076
22. B.C.M. Reis, A.J. dos Santos, N.F.S. Pereira et al., Effect of Nb addition on the machinability of a pearlitic gray cast iron. J. Mater. Eng. Perform. **31**(7), 5983–5999 (2022). https://doi.org/10.1007/s11665-022-06669-9
23. W. Sun, B. Wang, X. Liu et al., Controlling the tribology performance of gray cast iron by tailoring the microstructure. Tribol. Int. (2022). https://doi.org/10.1016/j.triboint.2021.107343
24. Q. Li, Y. Zhang, Y. Zhang et al., Influence of Sn and Nb additions on the microstructure and wear characteristics of a gray cast iron. Appl. Phys. A. (2020). https://doi.org/10.1007/s00339-020-03468-8
25. A. Bedolla-Jacuinde, E. Solis, B. Hernandez, Effect of niobium in medium alloyed ductile cast irons. Int. J. Cast Met. Res. **16**(5), 481–486 (2016). https://doi.org/10.1080/13640461.2003.11819625
26. L.I. Rivera, V.A. Roca, C.F. Patiño, C.M. Cruells, Microalloyed niobium influence on ductile ferrite cast irons. Int. J. Cast Metals Res. **16**(1–3), 65–70 (2003). https://doi.org/10.1080/13640461.2003.11819560
27. Z.F. Qijie, H. Zhai, Effect of Nb on structure and mechanical properties of chilled cast iron at room and elevated temperatures. J. Mater. Sci. Technol. **20**(03), 301 (2004)
28. W. Zhou, H. Zhu, D. Zheng et al., Niobium alloying effect in high carbon equivalent grey cast iron. China Found. **8**(1), 36–40 (2011)
29. Y. Zhu, J. Li, C. Zhang et al., High temperature dry tribological behavior of Nb-microalloyed bearing steel 100Cr6. Materials (Basel) (2021). https://doi.org/10.3390/ma14185216
30. J. Lacaze, Pearlite growth in cast irons: a review of literature data. Int. J. Cast Met. Res. **11**(5), 431–436 (2016). https://doi.org/10.1080/13640461.1999.11819312
31. A.O. Devecili, R. Yakut, The effect of Nb supplement on material characteristics of iron with lamellar graphite. Adv. Mater. Sci. Eng. **2014**, 1–5 (2014). https://doi.org/10.1155/2014/465947
32. M. Górny, M. Kawalec, Effects of titanium addition on microstructure and mechanical properties of thin-walled compacted graphite iron castings. J. Mater. Eng. Perform. **22**(5), 1519–1524 (2012). https://doi.org/10.1007/s11665-012-0432-8
33. X. Zhi, J. Xing, H. Fu et al., Effect of niobium on the as-cast microstructure of hypereutectic high chromium cast iron. Mater. Lett. **62**(6–7), 857–860 (2008). https://doi.org/10.1016/j.matlet.2007.06.084
34. J.P. Lai, Q.L. Pan, X.D. Wang et al., Effects of Nb on the microstructure and properties of Ti-added hypereutectic high-Cr cast iron. J. Mater. Eng. Perform. **27**(9), 4373–4381 (2018). https://doi.org/10.1007/s11665-018-3516-2
35. X. Zhi, Y. Han, J. Xing, Refining effect of Nb on hypereutectic high-chromium cast iron. Rare Met. Mater. Eng. **40**, 169–171 (2011)